Neurotoxicity Research (2020) 38:408–420
https://doi.org/10.1007/s12640-020-00233-w

ORIGINAL ARTICLE

# Maternal Hyperhomocysteinemia Induces Neuroinflammation and Neuronal Death in the Rat Offspring Cortex

A. D. Shcherbitskaia[1,2] · D. S. Vasilev[2] · Yu. P. Milyutina[1] · N. L. Tumanova[2] · I. V. Zalozniaia[1] · G. O. Kerkeshko[3] · A. V. Arutjunyan[1]

Received: 13 February 2020 / Revised: 19 May 2020 / Accepted: 29 May 2020 / Published online: 5 June 2020


## Abstract

Maternal hyperhomocysteinemia is one of the common complications of pregnancy that causes offspring cognitive deficits during postnatal development. In the present work, we evaluated the effect of prenatal hyperhomocysteinemia on structural and ultrastructural organization, neuronal and glial cell number, apoptosis (caspase-3 content and activity), inflammatory markers (tumor necrosis factor-α, interleukin-6, and interleukin-1β), and p38 mitogen–activated protein kinase (p38 MAPK) phosphorylation in the offspring brain cortex in early ontogenesis. Wistar female rats received methionine (0.6 g/kg body weight) by oral administration during pregnancy. Histological and biochemical analyses of 5- and 20-day-old pups' cortical tissue were performed. Lysosome accumulation and other neurodegenerative changes in neurons of animals with impaired embryonic development were investigated by electron microscopy. Neuronal staining (anti-NeuN) revealed a reduction in neuronal number, accompanied by increasing of caspase-3 active form protein level and activity. Maternal hyperhomocysteinemia also elevated the number of astroglial and microglial cells and increased expression of interleukin-1β and p38 MAPK phosphorylation, which indicates the development of neuroinflammatory processes.

**Keywords** Homocysteine · Neuroinflammation · Glial reaction · Parietal cortex · Neurodegeneration · Cytokines

### Abbreviations

| | |
|---|---|
| Hcy | Homocysteine |
| HHC | Hyperhomocysteinemia |
| IL-1β | Interleukin-1β |
| IL-6 | Interleukin-6 |
| p38 MAPK | p38 mitogen–activated protein kinase |
| PHHC | Prenatal hyperhomocysteinemia |
| TNF-α | Tumor necrosis factor alpha |

## Introduction

Homocysteine (Hcy) is a sulfur-containing amino acid formed by demethylation of methionine, the main methyl donor in mammals (Shafqat et al. 2013). Hcy metabolism is an interaction of several pathways: remethylation to methionine by 5-methyltetrahydrofolate-homocysteine methyltransferase, metabolism to cystathionine by cystathionine-β-synthase (Yi et al. 2000), and pathway which is linked to betaine by the enzyme betaine-homocysteine methyl transferase, providing Hcy with a methyl group for remethylation to methionine (Blom and Smulders 2011). Metabolic relation of methionine-homocysteine is of particular importance, since Hcy cannot be obtained from diet (Selhub 1999). Mutations in metabolic enzymes or deficiency in cofactors such as vitamin $B_6$, $B_{12}$, and folate can lead to increased levels of plasma Hcy, termed hyperhomocysteinemia (HHC) (Boldyrev 2009). HHC has been recognized as a major risk factor for various vascular diseases and neuronal degeneration (Kovalska et al. 2019; Ostrakhovitch and Tabibzadeh 2019). During pregnancy, several complications have been associated with HHC and elevated Hcy levels suggested to play a role in the etiology of

✉ A. D. Shcherbitskaia
nastusiq@gmail.com

[1] D.O. Ott Institute of Obstetrics, Gynecology, and Reproductology, St. Petersburg, Russia

[2] I.M. Sechenov Institute of Evolutionary Physiology and Biochemistry of the Russian Academy of Sciences, St. Petersburg, Russia

[3] Saint Petersburg Institute of Bioregulation and Gerontology, St. Petersburg, Russia

preeclampsia, placental abruption, intrauterine growth retardation, and neural tube defects (Hague 2003; Kasture et al. 2018).

Mechanisms of deleterious pleiotropic effects of HHC are far from being completely elucidated and assume the following: oxidative stress (Baydas et al. 2006), overstimulation of glutamate receptors (Boldyrev 2009; Sibarov et al. 2016), apoptosis (Baydas et al. 2005), and inhibition of NO-mediated signaling pathway (Wu et al. 2019), as well as DNA damage (Koz et al. 2010). Recent studies of acute and chronic administration of Hcy showed elevated concentration of proinflammatory cytokines such as tumor necrosis factor alpha (TNF-α), interleukin-1β (IL-1β), and interleukin-6 (IL-6) in serum, hippocampus, and cerebral cortex of mature rats (da Cunha et al. 2012; da Cunha et al. 2010).

Recent studies demonstrated that our model of chronic HHC (Arutyunyan et al. 2012) led to an increase in lipid peroxidation products (Pustygina et al. 2015), as well as pro-inflammatory cytokine IL-1β level in serum of pregnant animals and in their placenta indicating oxidative stress and systemic inflammatory reaction development (Arutjunyan et al. 2020). Mediators of neuroinflammation such as cytokines, growth factors, and reactive oxygen species are secreted to promote neuronal repair and maintenance, which in chronic status may be harmful to healthy tissue (Moore and O'Banion 2002). In addition, an increase in BDNF and NGF pro-form levels, which have an inhibitory effect on brain maturation in early ontogenesis (Barcelona and Saragovi 2015; Sasi et al. 2017) and, as a consequence, subsequent formation of cognitive functions, has been shown in the brain of fetuses after prenatal HHC (PHHC) (Arutjunyan et al. 2020).

The cerebral cortex is a particularly important structure for processing spatial learning and memory and, together with the hippocampus, participates in working memory organization. The development delay in these regions is responsible for cognitive deficiency. It was recently shown that pups with PHHC presented obvious pathological changes in hippocampal neurons' cell bodies, suggesting that the cell morphological changes caused by impaired maternal folate status may be, at least partly, associated with memory deficits in the rat offspring (Wang et al. 2018). Furthermore, we have reported that PHHC led to the disruption of cognitive function in mature offspring accompanied by a decrease in the content of biogenic amines and their metabolites in the hippocampus (Shcherbitskaya et al. 2017).

The neurotoxic effects of Hcy were extensively studied during postnatal life; however, little is still known about the consequences of its deleterious action in the prenatal period. Thus, in the present work, for the first time, we investigated the long-term effects of maternal HHC on the offspring brain development by evaluating the cortex morphology and ultrastructure. Our hypothesis is that biochemical changes induced in the fetal brain by PHHC can cause neuroinflammation and morphological changes in neuronal cells even after Hcy level normalization resulting in memory impairment in mature offspring.

## Materials and Methods

### Animals

Wistar rats were obtained from the Rappolovo Animal Center, Saint Petersburg region, Russia. Animals were housed at a constant room temperature with 12-h light and dark cycle and had free access to a 20% (w/w) protein commercial chow and clean drinking water throughout the study. Exclusion criteria included signs of illness and behavioral defects at the start of the study.

### Chronic Methionine Treatment

To confirm pregnancy, we verified the presence of sperm in the vaginal smears after mating the female rats. Then, they received daily administration of methionine (0.6 g/kg) in drinking water per os on days 4–21 of pregnancy. At the same time, control animals received water. Pups were killed at the postnatal (P) days 1, 3, 5, and 20. Day of birth was defined as P1. The treatment paradigm followed for the study is illustrated in Fig. 1.

### Homocysteine Content

Blood serum was separated by centrifugation (2000*g*, 10 min) and stored at − 80 °C. Brain tissues were homogenized on ice 1:1 (w/v) in a 0.001M PBS buffer (pH 7.4). Homogenates

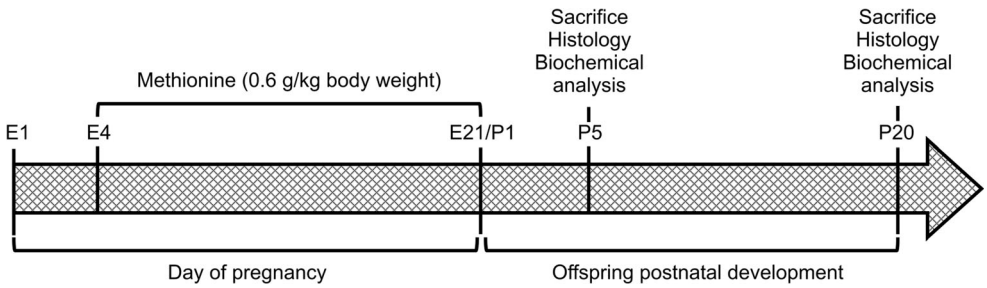


**Fig. 1** Treatment paradigm followed during the study

were then centrifuged at 16000*g* at 4 °C for 20 min, and the supernatants were used in the assay. Determination of total Hcy in the serum and whole brain supernatants of 1-, 3-, 5-, and 20-day-old pups was performed by the immunochemiluminescent method, using the Architect i1000 analyzer (Abbott, USA).

## Brain Tissue Preparation for Microscopy

On P5 and P20, the brain tissue structure of pups ($n = 8$) from control females was compared with that of offspring ($n = 8$) from females treated by methionine during pregnancy. The brain tissue blocks were fixed by perfusion of 4% paraformaldehyde solution in 0.1 M PBS (pH 7.4) at 4 °C for 2 weeks. Brain tissue was immersed in 20% sucrose solution in PBS (pH 7.4), then frozen and sectioned in the coronal plane using a Cryostat Leica CM 1510S (Leica Microsystems, Germany). We analyzed 20-μm sections of the parietal cortex in the blocks of brain tissue, starting at the level Bregma = − 4.5 mm (Paxinos and Watson 2007).

## Light Microscopy

Some slices were stained by cresyl violet (Nissl) and analyzed using an AF7000 microscope with DFC495 digital camera (Leica, Germany). The areas of interest are presented in Fig. 3e. The total number of slices analyzed was 10 per animal. The distance between analyzed slices was 40 μm.

## Immunochemistry

We also determined the number of cells labeled by neuronal (NeuN protein) and glial (GFAP, Iba1) marker proteins in the same area of the parietal cortex. For this, a sequence of sections (10 sections per animal with 80 μm between them) were randomly selected and used for immunolabeling.

Sections were incubated overnight at 37 °C in PBS containing 2% bovine serum albumin, 0.3% Triton X-100 (Merck, Darmstadt, Germany), and one of three antibodies: rabbit polyclonal anti-Fox3/NeuN (ab104224; Abcam, Bristol, UK; dilution 1:1000), rabbit polyclonal anti-GFAP (glial fibrillary acidic protein, ab7260, Abcam, 1:200) or rabbit anti-Iba1 (ionized calcium-binding adapter molecule, ab178846, Abcam, 1:100) antibody. After thorough rinsing, the sections were incubated for 1 h at 37 °C in florescent-tagged secondary antibodies: FITC-conjugated (ab97050, Abcam, 1:200) or PE-conjugated (ab7007, Abcam, 1:200) secondary antibody against rabbit IgG diluted in the blocking serum. Before mounting, brain sections were counterstained with Hoechst 33342 (Invitrogen, USA) to show cortical lamination and to aid in the total cell count. Microscopy was performed using a Leica DMR microscope connected to a Leica TCS SL confocal scanner (Leica Microsystems, Germany). A 488-nm wavelength He/Ar laser was used for excitation of FITC and PE, 350 nm for Hoechst 33342. Emissions from the FITC, PE, and Hoechst 33342 were observed in the 496–537-nm, 652–690-nm, and 430–461-nm wavelengths, respectively. The brightness of the cell bodies and nuclei was measured using the Video TesT-Morphology software program (Video TesT, Saint Petersburg, Russia). The immune-positive signal was analyzed if it was more than 300% of the background.

Cortical cells were analyzed in a 500-μm-wide section including layers II–VI. The number of NeuN-positive neurons, GFAP-positive astrocytes, and Iba1-positive microglial cells was counted in the same field of vision for each brain slice.

## Electron Microscopy

On P5 and P20, the ultrastructure of the parietal cortex (the same area as we used in the immunofluorescent analysis) was analyzed in PHHC and control pups. After perfusion (1% of glutaraldehyde, 1% formaldehyde in 0.1 M PBS, pH 7.4), brain tissue was fixed in 1% $OsO_4$, stained with uranyl acetate, dehydrated, and embedded in Araldite by the protocol described previously (Vasilev et al. 2018). Ultra-thin sections of 500-Å thickness were made using LKB-III (LKB, Sweden) and analyzed using an FEI Tecnai V2 (FEI, USA) transmission electron microscope. To evaluate the viability of neurons, the structural features of cortical cells were analyzed.

## Cytokines (TNF-α, IL-1β, and IL-6) Assay

The tissue of the cerebral cortex was homogenized in 1:5 (w/v) 0.001 M PBS (pH 7.4). The homogenate was centrifuged at 16000*g* for 20 min at 4 °C, and the supernatant was used in the assays. TNF-α, IL-1β, and IL-6 levels in the cerebral cortex were quantified by rat high-sensitivity enzyme-linked immunosorbent assays (ELISA) with commercially available kits as per instructions provided by the manufacturer (R&D Systems, USA). The content of these cytokines was measured through optical densitometry at 450 nm in the microplate reader (ELx800, BioTek Instruments, USA).

## Immunoblotting

Brain tissues were homogenized on ice 1:3 (w/v) in a 0.001 M PBS buffer (pH 7.4). Tissue homogenates were then centrifuged at 16000*g* at 4 °C for 20 min, and supernatants were collected into fresh tubes. Protein determinations in the homogenates were performed according to the Bradford method using bovine serum albumin as the standard. Proteins were separated by SDS-PAGE and transferred to PVDF membranes. Blots were washed three times for 10 min each in TBST-buffered saline (50 mM Tris-HCl; 150 mM NaCl; 0.1% Tween 20) and blocked with 2% bovine serum albumin

(Sigma-Aldrich Chem. Co., USA) in TBST-buffered saline for 1.5 h prior to application of the primary antibody. Blots were then incubated overnight at 4 °C with primary antibodies including rabbit monoclonal antibody against caspase-3 (9662S, Cell Signaling, 1:1000), p38 MAPK (8690L, Cell Signaling, 1:1000), and GAPDH (2118L, Cell Signaling, 1:1000), and mouse monoclonal antibody against phospho-p38 MAPK (9216L, Cell Signaling, 1:1000). The blots were washed and incubated for 1.5 h with a secondary antibody, goat anti-rabbit or anti-mouse Ig peroxidase conjugated (#1706515 or #1706516, Bio-Rad) at a dilution of 1:3000. Specific binding was detected using Clarity Western ECL Substrate (Bio-Rad, 170-5061). Bands were quantified by densitometry using a computerized software program (ImageLab, Bio-Rad). Based on the existing recommendations for normalization of the target protein content (Bass et al. 2017), the obtained data were normalized to the content of GAPDH; with total protein content in the gel determined using the stain-free technology (Bio-Rad) according to the manufacturer's instruction.

### Caspase-3 Activity

Caspase-3 activity was assayed in 20 mM HEPES, containing 0.1% CHAPS, 2 mM EDTA, and 5 mM DTT (pH 7.4) using 4 mM synthetic peptide Ac-DEVD-pNA (N-acetyl-Asp-Glu-Val-Asp p-nitroanilide) as a substrate. Samples containing 90 μg of protein were incubated at 37 °C for 10 min; the reaction was initiated by adding the substrate, and the absorbance of the reaction mixture was recorded at 405 nm at 37 °C every 5 min for 25 min. The activity of caspase-3 was defined as micromoles of the reaction product pNA per minute per milligram protein.

### Statistical Analysis

All values are expressed as mean ± standard error of the mean (SEM). The normality of the data was tested using the Shapiro-Wilk normality test. To verify the equality of variances, Levene's test was used. Statistical analysis was performed with STATISTICA 10.0. Variance was analyzed by the Mann-Whitney $U$ test and Student's $t$ test. Values of $p \leq 0.05$ were considered statistically significant.

## Results

### Homocysteine Content

Recently, we have shown that daily methionine administration leads to an increase in maternal serum Hcy level during pregnancy (Arutjunyan et al. 2020). Therefore, we only measured serum and brain content of Hcy in the offspring. The offspring from mothers with methionine administration had elevated serum Hcy concentrations up to P3 when compared with pups from control mothers (Mann-Whitney $U$ test $p \leq 0.05$; Fig. 2a). There was no difference in serum Hcy levels between the control offspring and pups after PHHC on P5 and P20. Figure 2 b shows that in the PHHC group of newborns cerebral Hcy concentration was approximately twofold higher than the normal content (Mann-Whitney $U$ test $p \leq 0.01$; Fig. 2b), but no difference between groups was observed on P3, P5, and P20. Thus, the normalization of Hcy content in the organism of experimental pups occurred by the age of P5.

### Light Microscopy

In early ontogenesis, a comparative study of the structural organization of the parietal cortex of pups subjected to PHHC was carried out using the Nissl method. On P5, in the parietal cortex of pups, some signs of destruction of nerve cells were detected in comparison with control animals (Fig. 3a, b). Part of the cortical neurons became swollen, lost their

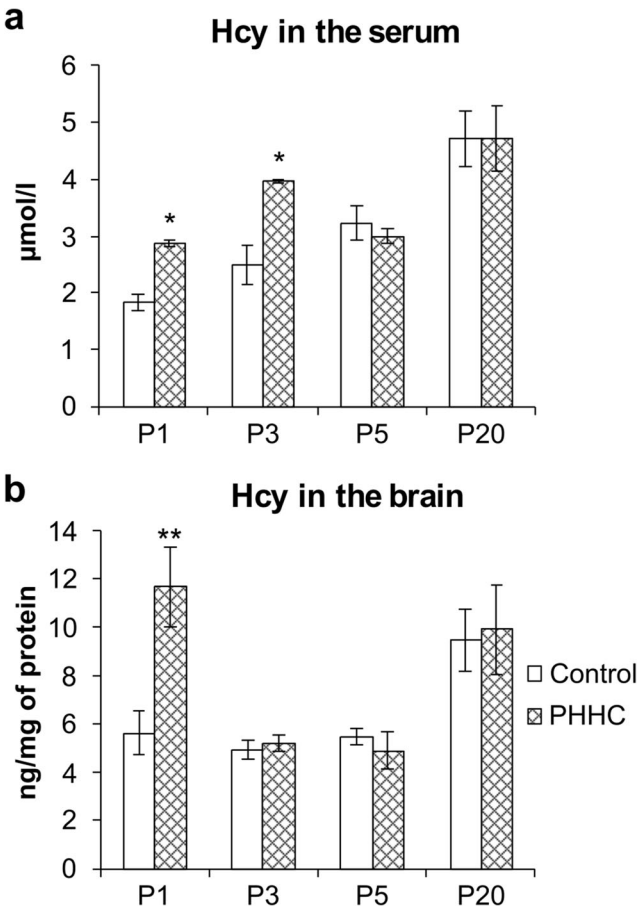


**Fig. 2** Effect of prenatal hyperhomocysteinemia on rat pup serum (a) and brain (b) total homocysteine concentrations. PHHC, prenatal hyperhomocysteinemia. Data represent mean ± SEM, $n = 8–9$ rats/group. Significance of difference between PHHC and control groups were determined by the Mann-Whitney $U$ test (asterisk indicates $p \leq 0.05$, and double asterisk indicates $p \leq 0.01$)

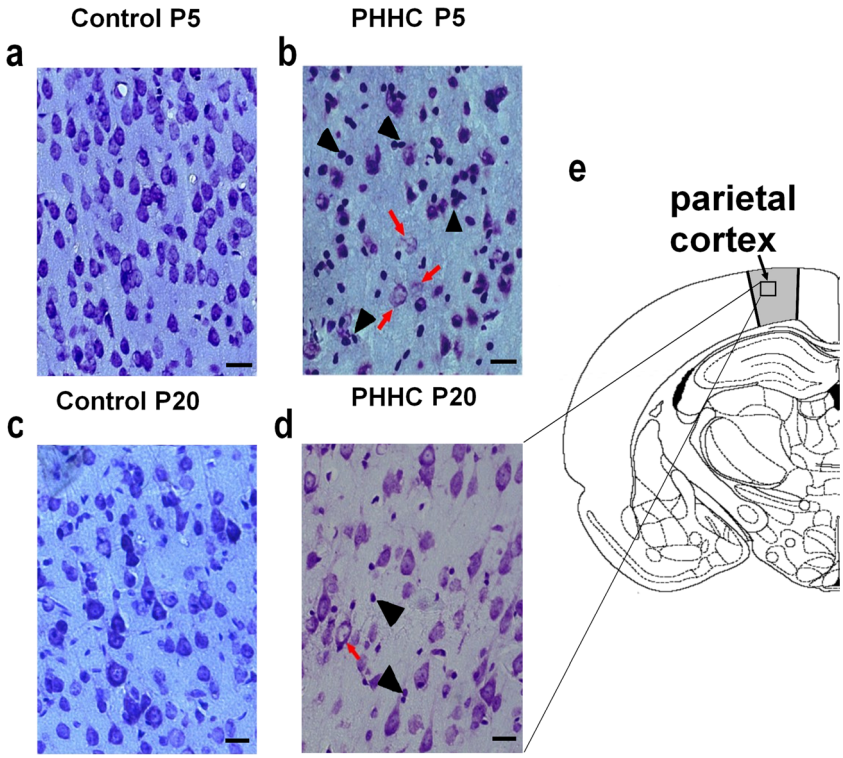


**Fig. 3** Tissue of the parietal cortex of rat pups in control (a, c) and after prenatal hyperhomocysteinemia (b, d) on P5 (a, b) and P20 (c, d). PHHC, prenatal hyperhomocysteinemia. Scale, 30 μm; Nissl staining. Red arrows, degenerating neurons; black arrowheads, glial cells. (e) Scheme of the analyzed area in the parietal cortex (gray shading)

shape, their processes, especially apical dendrites, became crimped. This type of degeneration is characteristic of cells in a state of chromatolysis. Numerous glial cells appeared in the neuropil. At P20, in rats from the PHHC group, the number of cortical neurons decreased compared with that in control animals (Fig. 3c, d). A large number of dying neurons surrounded by glial cells were observed in the neuropil (Fig. 3b, d).

## Quantitative Analysis

The parietal cortex cellular composition of rat pups in control and PHHC groups is presented in Fig. 4. The decrease in the number of viable cortical neurons expressing NeuN protein was observed in PHHC pups on P5 and P20 (Mann-Witney *U* test, $p \leq 0.05$ for 5-day-old rats, $p \leq 0.01$ for 20-day old). In P5 PHHC pups, the number of neurons was 61.8% of the control level, and it decreased to 23.8% on P20 (Fig. 4c). In addition, features of glial reaction were observed in the cortical tissue of PHHC pups (Fig. 4b). The number of glial cells increased relative to the control. In P5 PHHC pups, the average astrocyte number was 172.4% of the control level (Mann-Witney *U* test $p \leq 0.01$; Fig. 4d), while the number of microglia was 2.8 times higher than that in control (Student's *t* test $p \leq 0.01$; Fig. 4e). On P20, the glial reaction intensified: the amount of astroglia was 381.6% (Mann-Witney *U* test $p \leq 0.01$; Fig. 4d) of the control, and the amount of microglia was 3.6 times higher than that in the control level (Student's *t* test $p \leq 0.01$; Fig. 4e). Thus, in the parietal cortex of PHHC pups, the decrease in the number of neurons and a strong glial reaction were observed.

## Electron Microscopy

The cortical tissue of P5 PHHC pups as well as in the control group (Fig. 5a–c) was shown to be immature with a large intercellular space volume and numerous thin processes of neurons. Growth cones (Fig. 5c) were less common in the neuropil of PHHC pups than those in control animals. A great number of light round growth vesicles and vacuoles of various sizes and shapes were observed in such growth cones. Some of them accumulated small bubbles similar to synaptic ones at one of their poles. In such places, densities were noticeable on the synaptic membranes. Cell contacts in the form of desmosomes predominated, while spines (Fig. 5g) and immature synaptic contacts were rare. Small neurons were located in groups. Their oval nuclei contained dispersed chromatin. Unlike the control group, in P5 PHHC pups, the large swollen neurons with numerous single ribosomes and those combined into numerous polysomes were observed (Fig. 5e, f). The endoplasmic reticulum was hypertrophically expanded (Fig. 5e), and numerous ribosomes were located on the surface of their tubules. Often, numerous lysosomes were found in the cytoplasm of such swollen neurons (Fig. 5d).

In cortical tissue of P20 PHHC pups as well as in control, the volume of intercellular space and the number of growth

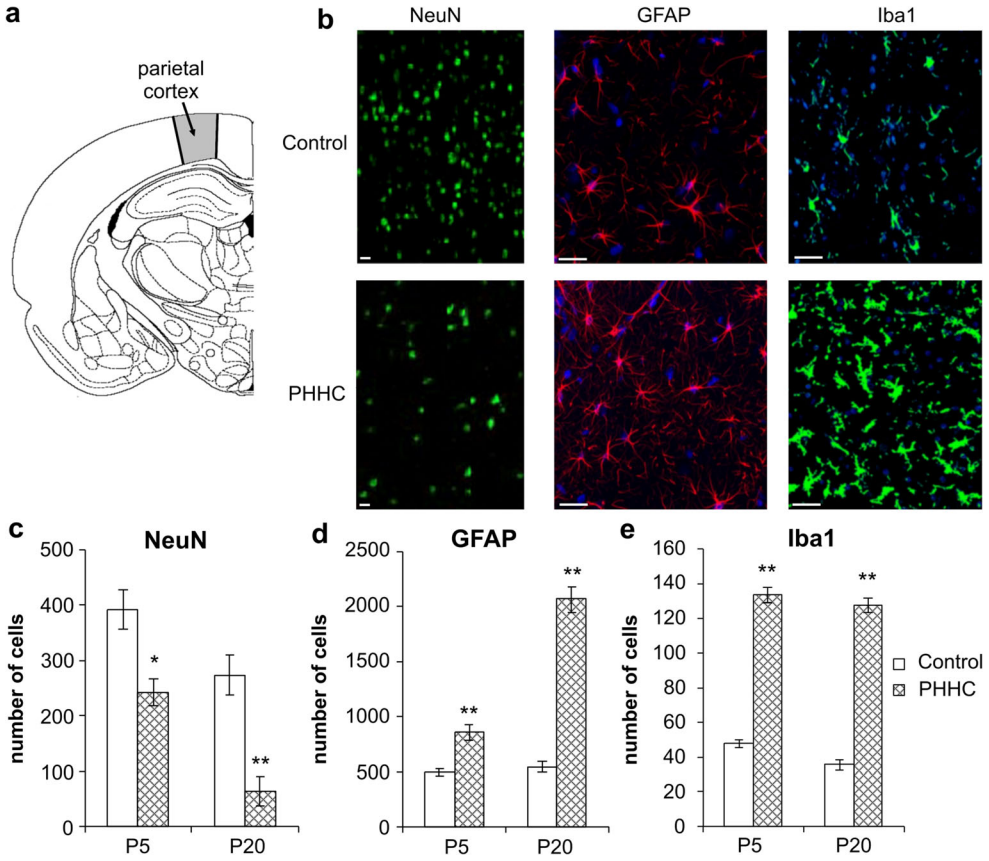


**Fig. 4** Effect of prenatal hyperhomocysteinemia on the neuronal and glial cell number in the parietal cortex of rats. PHHC, prenatal hyperhomocysteinemia. (a) Scheme of the analyzed area in the parietal cortex (gray shading). (b) Micrographs of the parietal cortex in control animals and pups subjected to PHHC 20 days after birth. Immunohistochemical staining of neuronal marker protein NeuN (FITC, left), marker of astrocytes GFAP (PE, in the middle), or microglial marker Iba1 (FITC, right). Cell nuclei were stained with non-specific nucleus dye DAPI (blue). Scale, 50 μm. The average number of cells in the parietal cortex: NeuN-positive neurons (c), GFAP-positive (d), and Iba1-positive (e) glial cells in control animals on P5 and P20 (white bars, $n = 8$) and PHHC (gray bars, $n = 8$). Values are expressed as mean ± SEM. Asterisks indicate statistically significant (*t* test or the Mann-Whitney *U* test) differences PHHC versus control (asterisk indicates $p \leq 0.05$, and double asterisk indicates $p \leq 0.01$)

cones decreased compared with those of P5 pups (Fig. 6a, b). Dendrites with dendritic tube branches, mature synapses, and dendritic spines without a spine apparatus (Fig. 6c) appeared to be more numerous. There was some deference in cortical ultrastructure between control and PHHC groups. Numerous ribosomes, especially in rough EPR, were observed in the PHHC group of pups (Fig. 6b). Some neurons were swollen, with swollen and hypertrophically enlarged EPR channels (Fig. 6b). These signs are characteristic of cells in a state of chromatolysis, which was observed in PHHC brain slices stained by the Nissl method (Fig. 3b, d). Lysosomes were found in PHHC pups more often than those in control, not only in the cytoplasm of neurons, but also in dendrites (Fig. 6f). Some neurons were surrounded by glial cells and overgrown glial processes. The group of glial cells can be seen in Fig. 6g. In neurons with small sizes, wrinkling of the cell bodies and their processes took place, and the cytoplasm became more electron-dense (or hyperchromic, see Fig. 6d).

## Effect of PHHC on the IL-1β, IL-6, and TNF-α Content

The protein levels of proinflammatory cytokines are depicted in Fig. 7. The IL-1β expression was significantly increased in the cortex (1.5-fold, Student's *t* test $p \leq 0.01$) of PHHC rats on P20 as compared with that of the controls. There was no significant difference in concentrations of IL-6 and TNF-α between the PHHC and control groups of pups on P5 and P20.

## p38 MAPK Content

PHHC increased the p38 MAPK phosphorylation in the cortex of rats on P5 (1.59-fold, Student's *t* test $p \leq 0.05$), despite the fact that the total levels of p38 MAPK were not altered (Fig. 8b). Furthermore, the ratio of phospho-p38 and total p38 MAPK content was also elevated in the PHHC group of pups on P5 (Fig. 8c). The levels of these proteins were quantified in the rat cortex on P20, but no difference between groups was observed (Fig. 8b, c).

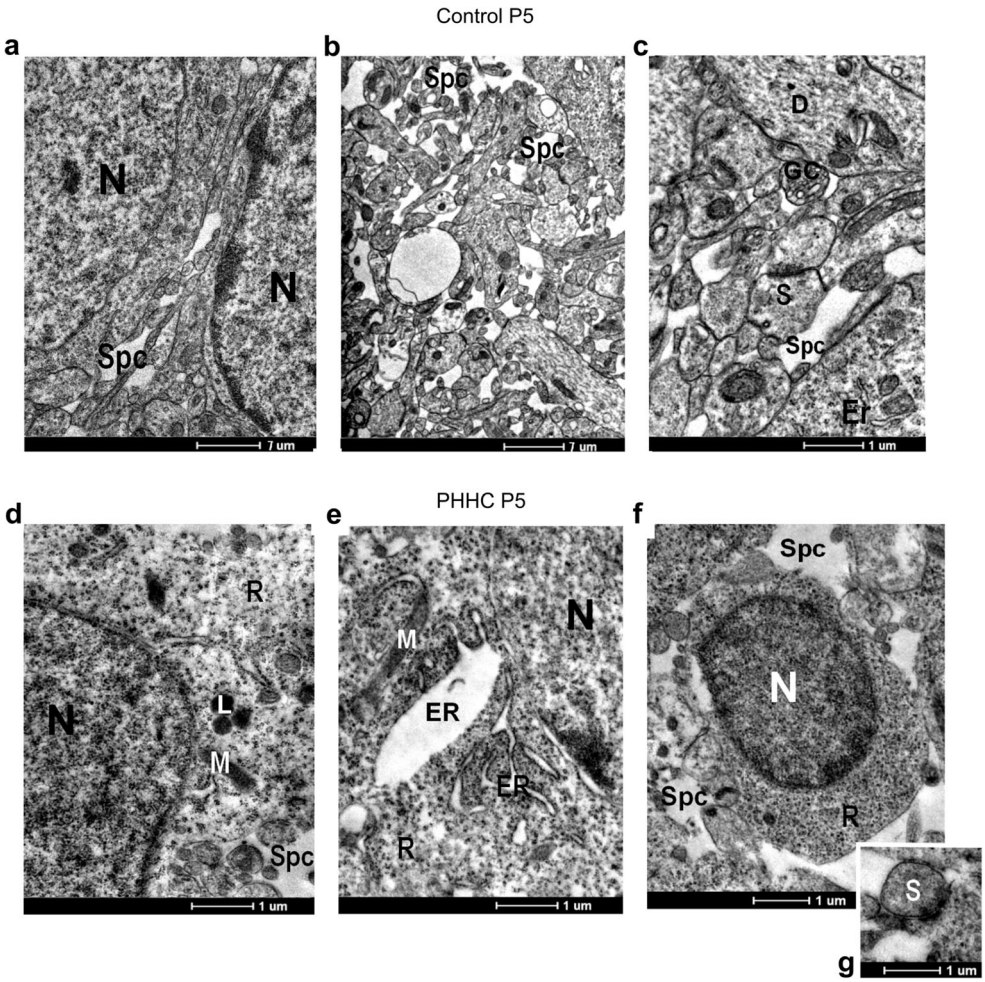


**Fig. 5** Representative ultrastructural images of the parietal cortex of 5-day-old pups in control (a–c) and after prenatal hyperhomocysteinemia (d–g). PHHC, prenatal hyperhomocysteinemia. Electron microscopy. N, nucleus; D, dendritic processes; GC, growth cone; Spc, intercellular space; L, lysosomes; M, mitochondria; ER, endoplasmic reticulum; R, ribosomes; S, synaptic contact. (g) Axo-spine synaptic contact

### Caspase-3 Content and Activity

Expression of caspase-3 active form (p17) as well as its ratio to procaspase-3 (p35) was higher (1.40- and 1.46-fold, respectively, Student's $t$ test $p \leq 0.05$) in the cortex of P5 pups, whose mothers received methionine (Fig. 8d). However, examination of two forms of caspase-3 (p17 and p35) by western blot revealed that their content in the brain cortex of the PHHC group did not differ from control on P20 (Fig. 8d).

An increase in the caspase-3 activity (evaluated as an increased rate of reaction product accumulation) was observed in the brain cortex of pups on P20 in the PHHC group ($2.54 \pm 0.17$ μmol pNA per min per mg protein vs. $1.79 \pm 0.14$ μmol pNA per min per mg protein in the control group; the Mann-Whitney $U$ test $p \leq 0.05$) (Fig. 8e). The caspase-3 activity on P5 only showed a tendency to increase in the group of pups after PHHC.

## Discussion

Increased Hcy level in the mother's blood is one of the pathological factors that can disrupt fetal brain development during the embryonic period. Hcy negatively affects the embryonic brain, not only via disruption of the functioning of the maternal organism, but also by acting directly on the fetus, due to its ability to penetrate through the placental barrier (Tsitsiou et al. 2011). Our previous studies showed that oral methionine administration significantly increased the level of Hcy in the serum of pregnant rats (Arutjunyan et al. 2020), which according to the literature data correlated with the Hcy level in newborns (Murphy et al. 2004). The present work demonstrated that PHHC increased the total Hcy level in the serum of newborn rat pups on P1 more than 1.5-fold. The data obtained are consistent with our previous results about elevated Hcy level in the blood and brain of fetuses that underwent PHHC (Arutjunyan et al. 2020), with increased Hcy level in pups from mothers with vitamin B–deficient diet observed by another group of researchers (Blaise et al. 2007). However, it is worth mentioning that significant differences in the level of Hcy were observed up to the 3rd day of postnatal life, most likely due to the consumption of accumulated Hcy with breast milk. We can assume that the decrease of Hcy content to normal level during ontogenesis is associated with no disturbance of the methionine cycle of rat pups during

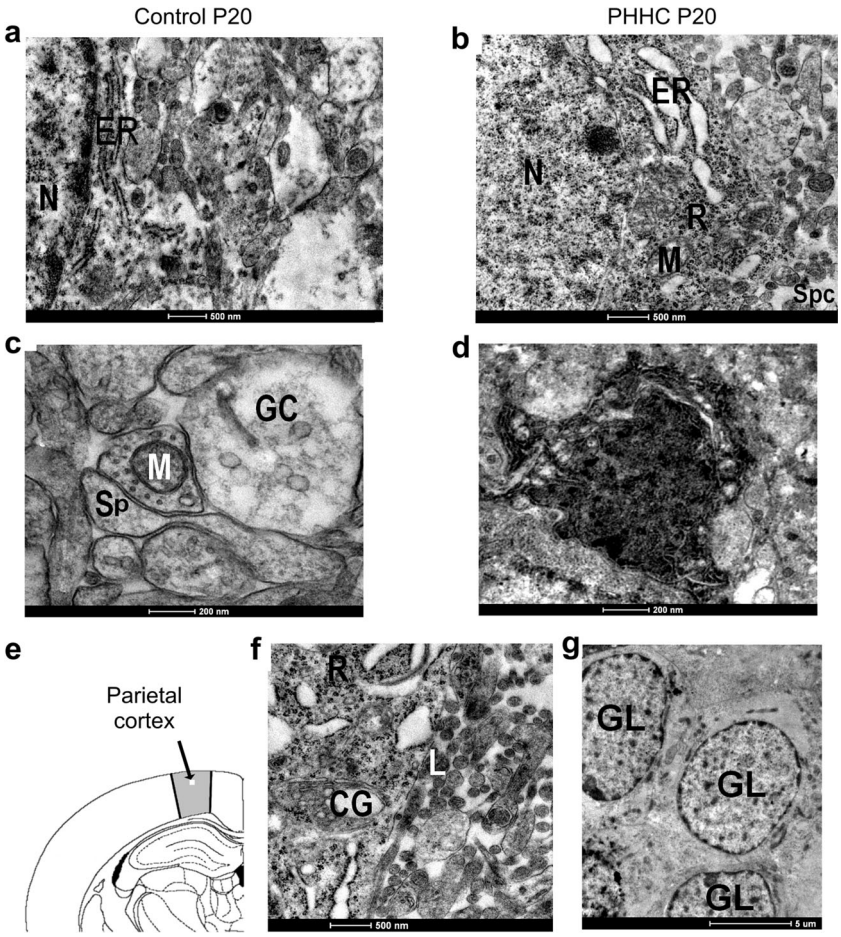


**Fig. 6** Representative ultrastructural images of the parietal cortex of 20-day-old pups in control (a, c) and after prenatal hyperhomocysteinemia (b, d, f, g). PHHC, prenatal hyperhomocysteinemia. Electron microscopy. N, nucleus; GC, growth cone; L, lysosomes; M, mitochondria; ER, endoplasmic reticulum; CG, Golgi complex; R, ribosomes; Sp, dendritic spine; GL, glial cell; Spc, intercellular space. (e) The area of parietal cortex analyzed by electron microscopy. Scale: (a, b, f) 500 nm; (c, d) 200 nm; (g) 5 μm

embryogenesis and its normalization with the transition of mothers to standard diet after birth.

There is an evidence that Hcy accumulates in such regions of the brain as the cerebellum, hippocampus, and striatum of animals born to mothers with experimental HHC during pregnancy and lactation (Blaise et al. 2007; Chung et al. 2003). Furthermore, an increase in Hcy content was observed in the pyramidal cells of the hippocampus, as well as in the granular cells of the dentate gyrus of mice with genetic HHC (Chung et al. 2003). Consequently, there is a reason to believe that PHHC can lead to an increase in the level of Hcy in the cerebral cortex of the developing embryo. In this study, we also found an elevation in Hcy content in the brains of newborn rats that, along with a prenatal effect of maternal HHC, could contribute to the increased neuronal cell death.

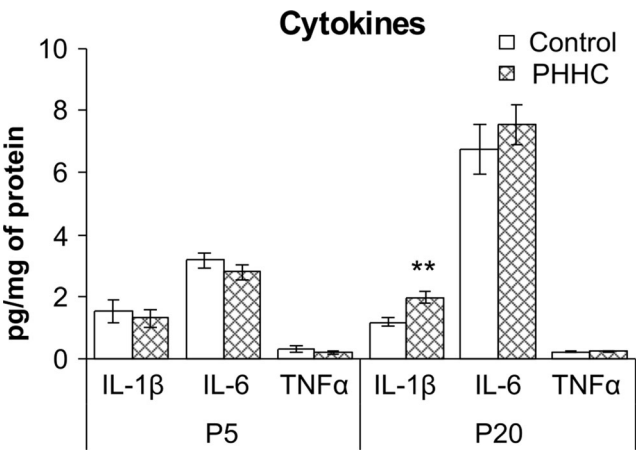


**Fig. 7** Effect of maternal hyperhomocysteinemia on cytokine content in the rat pup cerebral cortex. PHHC, prenatal hyperhomocysteinemia. Data represent mean ± SEM; $n = 9$ rats/group. Significance of difference between PHHC and control groups were determined by Student's $t$ test (double asterisk indicates $p \leq 0.01$, and asterisk indicates $p \leq 0.05$)

To confirm this assumption, we performed a light and electron microscopic analysis that showed morphological alterations in the nervous tissue of rats caused by PHHC. Thus, some ultrastructural features of neurodegeneration and neuronal cell death were observed in PHHC pups. Our data are in line with the reports of other authors that Hcy induces an appearance of swollen neurons with hypertrophically enlarged EPR channels and accumulation of ribosomes in the cytoplasm (Figueiro et al. 2019; Schweinberger et al. 2018a). The swollen neurons (chromatolysis) were observed in different models of brain pathology, but the mechanisms of structural changes in such neurons are poorly understood. The

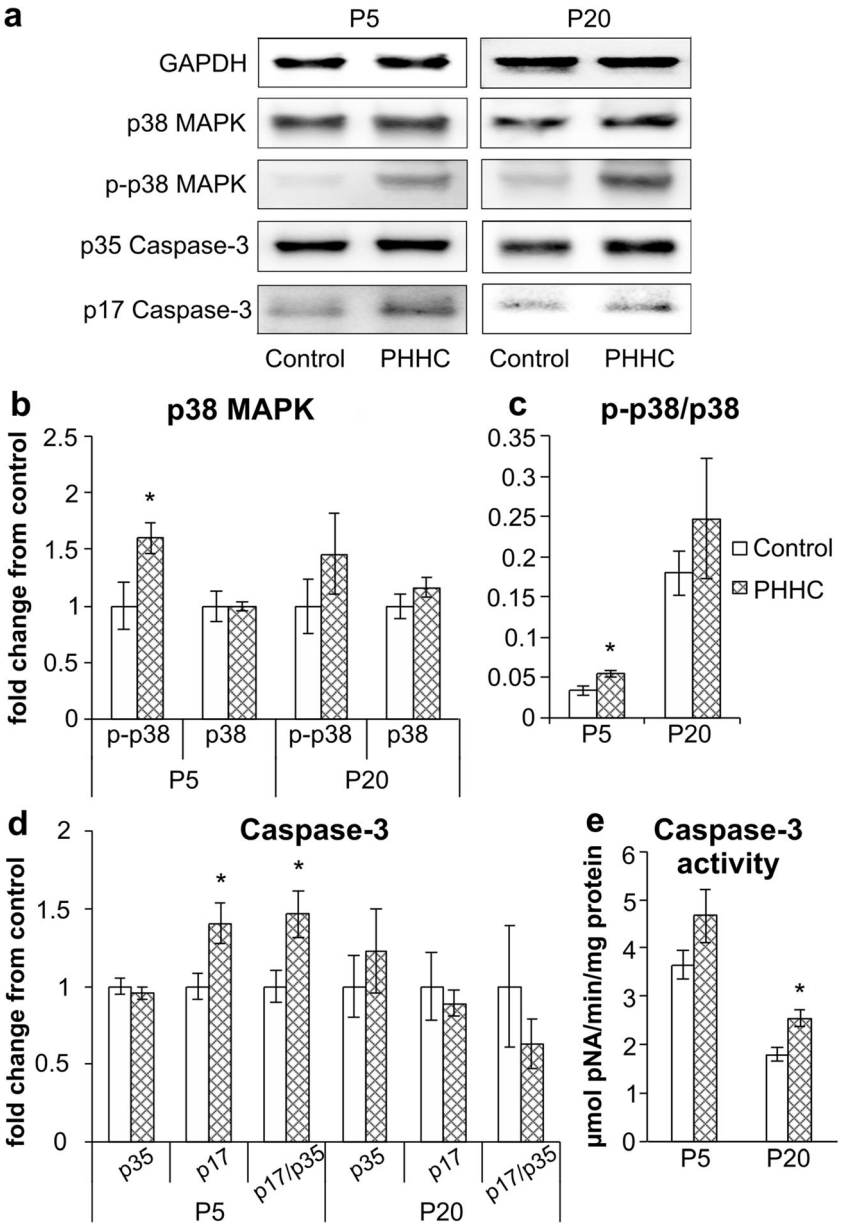


**Fig. 8** Effects of maternally induced hyperhomocysteinemia on the expression level of p38 and phospho-p38 MAPK (p-p38) and caspase-3 (p17 and p35) in the cerebral cortex of pups on P5 and P20. PHHC, prenatal hyperhomocysteinemia. (a) Representative western blots are shown for each condition. Band density (b) and ratio (c) of phospho-p38 and total p38 MAPK content in the brain cortex of rats determined by densitometry analysis. (d) Band density and ratio of p17 to p35 caspase-3 content in the brain cortex of rats determined by densitometry analysis. (e) Caspase-3 activity in the brain cortex of rats on P5 ($n = 7$–8) and P20 ($n = 9$–10) in control and PHHC groups. Data represent mean ± SEM; $n = 4$–9 rats/group. Significance of difference between PHHC and control groups were determined by Student's $t$ test or the Mann-Whitney $U$ test (asterisk indicates $p \leq 0.05$)

increase in the cell body volume is usually associated with the volume regulation disturbances. Some neurons contained swollen and hypertrophically enlarged EPR channels with numerous ribosomes, which was described in the other work as a characteristic feature of degenerated neurons (Castejón 2019). The accumulation of ribosomes in the cytoplasm, especially their polysomic forms, is known to be associated with neuronal viability and might suggest subsequent neuronal death (Riancho et al. 2014). In some experimental models of axotomy and neurotoxicity, it was shown that chromatolysis might be a reversible dysfunction of protein synthesis machinery, indicating the activation of neuroprotective mechanisms leading to neuronal function recovery (Palanca et al. 2014). Therefore, changes in the ribosome number and distribution observed in cortical neurons of PHHC pups might be associated with restorable changes of EPR rather than with neuronal death. On the other hand, the decrease in the number of cortical neurons accompanied by the increase in the cleaved caspase-3 protein content and activity observed in this work and our previous study (Arutjunyan et al. 2020) strongly suggest the presence of neuronal death in cortical tissue of PHHC pups.

It should be noted that the first month after birth is known to be a crucial period for the further functioning of neuronal networks in rodents, since neuronal maturation, synaptic pruning, cell elimination, myelination, synaptogenesis, and apoptosis take place in this period (Molnar and Clowry 2012). A substantial level of apoptosis during early postnatal development allows to remove the excess of neurons in some structures and to establish right connections between brain cells

(Costa et al. 2016). However, excessive apoptosis during development and subsequently adulthood can be detrimental (Nijhawan et al. 2000). Similar to our findings, Hcy-induced histological changes in neurons were described by another group of researchers. However, the focus of their study was directed to a loss of organelles and changes in the number of neurons in the whole brain (Schweinberger et al. 2018a). The treatment of adult rats with Hcy revealed a significant reduction in the number of neuronal cells, as well as in the number of dendritic spines, indicating neurodegeneration (Salissou et al. 2018). Hcy was shown to promote an increase in neuronal death in the cerebral cortex slices (Longoni et al. 2016). Most authors associated Hcy neurotoxicity with DNA damage (Koz et al. 2010), DNA methylation cycle disturbance (James et al. 2002; Yi et al. 2000), formation of reactive oxygen species, activation of apoptotic processes via mitochondria-mediated pathway (Baydas et al. 2006; Baydas et al. 2005), and excitotoxic mechanisms (Boldyrev 2009), whereas the role of neuroinflammatory mechanisms in Hcy effects is still poorly understood.

Glial cell activation is a feature of nerve tissue injury or stress, characterized by changes in morphology and the number of glial cells. Hcy effects on glial cells seem to be dose-dependent. High Hcy concentrations (> 1 mM) led to its cytotoxic effect, manifested in apoptosis and necrosis of glial cells (Wan et al. 2016), while lower concentrations (≤ 300 μM) increased proliferation and caused the neuroinflammatory reaction in astrocyte and microglial cell cultures (Longoni et al. 2018; Wan et al. 2016). Astrocytes treated with Hcy presented stress fiber reorganization, as well as rearrangement of the GFAP filament distributed along the cytoplasm and processes (Longoni et al. 2018). Similarly, another study using the HHC model in adult rats demonstrated a decreased projection number and shorter length with an increased cell body in astrocytes and microglia (Kumar and Sandhir 2019). The protein levels of GFAP and S100B (major astrocyte maturation markers) were shown to be markedly lower in the total brain of newborn pups after PHHC, suggesting impaired astrocytic fetal brain maturation (Baydas et al. 2007). We also used GFAP as a marker of astrocytes and observed a significant increase in the number of GFAP-positive cells in the cerebral cortex of rat pups on both P5 and P20. The controversy in the data might be associated with a difference in experimental designs of the PHHC model, animal age (P5–P20 vs. newborn), and technique of GFAP determination (immunohistochemistry vs. immunoblotting). Furthermore, Hcy significantly increased the content of GFAP and proinflammatory markers (IL1-β and TNFα) in the adult rat model of HHC (Salissou et al. 2018). Besides, the quantities of GFAP protein in the cell might vary depending on the maturation of glial cells (Middeldorp and Hol 2011), as well as on the remodeling of their cytoskeleton (Kumar and Sandhir 2019). The changes in the number of glial cells, especially microglia, are known to be a relevant feature of gliosis, as well as the glia activation in neuroinflammatory processes (Middeldorp and Hol 2011). The present study demonstrates that PHHC promotes proliferation and activation of microglia and astrocytes.

The activated glial cells produce various pro- and anti-inflammatory cytokines, which are thought to be important for immune cell infiltration and their activity coordination in brain tissues (Morale et al. 2006). It is well known that activation of microglia, which is a specialized form of macrophage residing the CNS, plays a crucial role in the activation of neuroinflammation (Craft et al. 2005; Moore and O'Banion 2002). Activated microglia cells produce and release some proinflammatory factors, such as NO, TNF-α, and IL-1β, in turn increasing oxidative stress and leading to further neuronal cell death (Wojtera et al. 2005). On the other hand, an increased reactive oxygen species production through p38 MAPK signaling pathway activation may cause energy metabolism impairment and contribute to inflammatory responses (Jha et al. 2015). In our previous work, oxidative stress was demonstrated in the brain of the offspring from mothers with methionine administration during gestation (Pustygina et al. 2015), so in this study, we evaluated the effect of PHHC on cytokine content in the rat pup cerebral cortex. The level of IL-1β but not TNF-α and IL-6 was increased in the rat cortex on P20 after PHHC, suggesting a proinflammatory response. Previous studies have shown that daily methionine injections during gestation did not alter TNF-α and IL-6 levels in the whole brain of 21-day-old rat offspring (Schweinberger et al. 2018b); however, the concentration of IL-1β was not determined. Some region specificity for cytokine response has been demonstrated for mild HHC effect since TNF-α, IL-1β, and IL-6 levels were shown to be increased in the hippocampus of female rats, with IL-1β and IL-6 content elevated in the cerebral cortex (Scherer et al. 2014). Another study demonstrated that microglial cells treated with Hcy in vitro had a noticeable increase in the proinflammatory marker IL-1β and a slight but nonsignificant increase in TNF-α (Weekman et al. 2017).

Neuroinflammation as well as Hcy elevation has been identified as a factor that contributes to the development of neurological diseases, such as Alzheimer's disease (Heneka et al. 2015), Parkinson's disease (Stojkovska et al. 2015), Huntington's disease (Chang et al. 2015), and multiple sclerosis (Frohman et al. 2006). Hcy has been reported to promote neuroinflammatory events, such as glial cell activation and production of proinflammatory cytokines in the brain of adult HHC animals (Chen et al. 2017; Kumar and Sandhir 2019; Weekman et al. 2019). However, studies of the inflammatory processes development in the offspring after PHHC are rare and seem to be ambiguous. The increase in the number of glial cells and their processes, numerous lysosomes in neuronal cells, and elevation of proinflammatory cytokine content

observed for the first time in our knowledge in the present study may indicate the role of neuroinflammation in cortical tissue development impairment of PHHC pups.

p38 MAPK is involved in the regulation of various cellular activities in CNS such as proliferation, differentiation, apoptosis, or survival in response to a wide range of extracellular stimuli including oxidative stress and proinflammatory cytokines (Kim and Choi 2015). The central role of p38 MAPK in many neural diseases has been proposed. The activation of p38 MAPK is involved in the microglia activation and neuroinflammation in the neurodegenerative disorders such as Alzheimer's and Parkinson's diseases (Jha et al. 2015; Lee and Kim 2017), as well as the dendritic spine loss observed in epilepsy and dementia that might be accompanied with the memory impairment (Yasuda et al. 2011). Under the influence of chronic stress conditions, p38 MAPK also activates the neuroinflammatory signaling pathway (Song et al. 2018). Several studies have reported that CNS proinflammatory cytokine overproduction and release activated by p38 MAPK contribute to neuronal damage (Bachstetter and Van Eldik 2010; van der Bruggen et al. 1999). p38 MAPK phosphorylation increased in the hippocampus and brain cortex under hypoxic conditions (Bu et al. 2007), and hypoxic p38 MAPK activation coincided with neuronal apoptosis and cognitive function declining in young rats (Zhu et al. 2020). Hcy was shown to activate p38 MAPK via NMDA receptors (Poddar et al. 2017; Poddar and Paul 2013), which in turn promotes the generation of reactive oxygen species resulting in microglia proliferation and activation (Zou et al. 2010). We have shown that phosphorylated p38 MAPK level was markedly increased in the rat pups cortex on P5, at the time when blood and brain Hcy levels were normalized after PHHC. Together with the morphological evidences, these data may suggest the involvement of p38 MAPK activation in PHHC-induced remote neural effects such as inflammation processes, apoptosis, and nervous tissue development delay.

It should be noted that morphological and biochemical changes in rat offspring cortex were observed after normalization of the level of Hcy in their organism. This provides further evidence that PHHC not only has short-time effects on the neuronal tissue but also causes long-term injury in the cortex and other brain regions resulting in memory impairment in mature offspring. In the framework of the present study, the proinflammatory cytokine analysis in combination with histological examination of the cerebral cortex complements the data published and allows us to suggest the involvement of neuroinflammatory processes in the pathogenesis of PHHC.

**Code Availability** Video TesT-Morphology (Video TesT), ImageLab (Bio-Rad), STATISTICA 10.0 (Statsoft), Xara Xtreme Pro 5 (Xara Group).

**Authors' Contributions** All authors contributed to the study conception and design. Material preparation and data collection and analysis were performed by Anastasiia Shcherbitskaia, Dmitrii Vasilev, Yulia Milyutina, Natalia Tumanova, Gleb Kerkeshko, and Irina Zalozniaia. The first draft of the manuscript was written by Anastasiia Shcherbitskaia and Alexander Arutjunyan. All authors commented on previous versions of the manuscript. All authors read and approved the final manuscript.

**Funding Information** The reported study was funded by the Russian Fund for Basic Research (research projects ##18-015-00099, 20-015-00388) and Russian state budget assignment for D.O. Ott Research Institute of Obstetrics, Gynecology and Reproductology (#AAAA-A19-119021290116-1). The study of the ultrastructure of nerve tissue was conducted as part of the Russian state budget assignment for I.M. Sechenov Institute of Evolutionary Physiology and Biochemistry of the Russian Academy of Sciences (#AAAA-A18-118012290373-7).

**Data Availability** The data that support the findings of this study are available from the corresponding author upon reasonable request.

## Compliance with Ethical Standards

**Conflict of Interest** The authors declare that they have no conflict of interest.

**Ethical Approval** All experiments were performed with the permission of the Ethics Committee of D.O. Ott Institute of Obstetrics, Gynecology and Reproductology and according to the European Communities Council Directive #86/609 for the Care of Laboratory Animals.

## References

Arutjunyan AV, Milyutina YP, Shcherbitskaia AD, Kerkeshko GO, Zalozniaia IV, Mikhel AV (2020) Neurotrophins of the fetal brain and placenta in prenatal hyperhomocysteinemia. Biochem Mosc 85: 248–259. https://doi.org/10.1134/S000629792002008X

Arutyunyan AV, Milyutina YP, Zaloznyaya IV, Pustygina AV, Kozina LS, Korenevskii AV (2012) The use of different experimental models of hyperhomocysteinemia in neurochemical studies. Neurochem J 6:71–76. https://doi.org/10.1134/s1819712411040027

Bachstetter AD, Van Eldik LJ (2010) The p38 MAP kinase family as regulators of proinflammatory cytokine production in degenerative diseases of the CNS. Aging Dis 1:199–211

Barcelona PF, Saragovi HU (2015) A pro-nerve growth factor (proNGF) and NGF binding protein, alpha2-macroglobulin, differentially regulates p75 and TrkA receptors and is relevant to neurodegeneration ex vivo and in vivo. Mol Cell Biol 35:3396–3408. https://doi.org/10.1128/MCB.00544-15

Bass JJ, Wilkinson DJ, Rankin D, Phillips BE, Szewczyk NJ, Smith K, Atherton PJ (2017) An overview of technical considerations for western blotting applications to physiological research. Scand J Med Sci Sports 27:4–25. https://doi.org/10.1111/sms.12702

Baydas G, Reiter RJ, Akbulut M, Tuzcu M, Tamer S (2005) Melatonin inhibits neural apoptosis induced by homocysteine in hippocampus of rats via inhibition of cytochrome c translocation and caspase-3 activation and by regulating pro- and anti-apoptotic protein levels. Neuroscience 135:879–886. https://doi.org/10.1016/j.neuroscience.2005.05.048

Baydas G, Ozer M, Yasar A, Koz ST, Tuzcu M (2006) Melatonin prevents oxidative stress and inhibits reactive gliosis induced by

hyperhomocysteinemia in rats. Biochemistry (Mosc) 71S1:S91–S95. https://doi.org/10.1134/s0006297906130153

Baydas G, Koz ST, Tuzcu M, Nedzvetsky VS, Etem E (2007) Effects of maternal hyperhomocysteinemia induced by high methionine diet on the learning and memory performance in offspring. Int J Dev Neurosci 25:133–139. https://doi.org/10.1016/j.ijdevneu.2007.03.001

Blaise SA, Nedelec E, Schroeder H, Alberto JM, Bossenmeyer-Pourie C, Gueant JL, Daval JL (2007) Gestational vitamin B deficiency leads to homocysteine-associated brain apoptosis and alters neurobehavioral development in rats. Am J Pathol 170:667–679. https://doi.org/10.2353/ajpath.2007.060339

Blom HJ, Smulders Y (2011) Overview of homocysteine and folate metabolism. With special references to cardiovascular disease and neural tube defects. J Inherit Metab Dis 34:75–81. https://doi.org/10.1007/s10545-010-9177-4

Boldyrev AA (2009) Molecular mechanisms of homocysteine toxicity. Biochemistry (Mosc) 74:589–598. https://doi.org/10.1134/s0006297909060017

Bu X, Huang P, Qi Z, Zhang N, Han S, Fang L, Li J (2007) Cell type-specific activation of p38 MAPK in the brain regions of hypoxic preconditioned mice. Neurochem Int 51:459–466. https://doi.org/10.1016/j.neuint.2007.04.028

Castejón OJ (2019) Electron microscopy study of nerve cell death types in some central nervous system diseases. A Review. Am J Biomed Sci & Res 3:73–83. https://doi.org/10.34297/ajbsr.2019.03.000637

Chang KH, Wu YR, Chen YC, Chen CM (2015) Plasma inflammatory biomarkers for Huntington's disease patients and mouse model. Brain Behav Immun 44:121–127. https://doi.org/10.1016/j.bbi.2014.09.011

Chen S, Dong Z, Cheng M, Zhao Y, Wang M, Sai N, Wang X, Liu H, Huang G, Zhang X (2017) Homocysteine exaggerates microglia activation and neuroinflammation through microglia localized STAT3 overactivation following ischemic stroke. J Neuroinflammation 14:187. https://doi.org/10.1186/s12974-017-0963-x

Chung YH, Hong JJ, Shin CM, Joo KM, Kim MJ, Cha CI (2003) Immunohistochemical study on the distribution of homocysteine in the central nervous system of transgenic mice expressing a human Cu/Zn SOD mutation. Brain Res 967:226–234. https://doi.org/10.1016/s0006-8993(03)02238-8

Costa AP, Lopes MW, Rieger DK, Barbosa SG, Goncalves FM, Xikota JC, Walz R, Leal RB (2016) Differential activation of mitogen-activated protein kinases, ERK 1/2, p38(MAPK) and JNK p54/p46 during postnatal development of rat hippocampus. Neurochem Res 41:1160–1169. https://doi.org/10.1007/s11064-015-1810-z

Craft JM, Watterson DM, Van Eldik LJ (2005) Neuroinflammation: a potential therapeutic target. Expert Opin Ther Targets 9:887–900. https://doi.org/10.1517/14728222.9.5.887

da Cunha AA, Ferreira AG, Wyse AT (2010) Increased inflammatory markers in brain and blood of rats subjected to acute homocysteine administration. Metab Brain Dis 25:199–206. https://doi.org/10.1007/s11011-010-9188-8

da Cunha AA, Ferreira AG, Loureiro SO, da Cunha MJ, Schmitz F, Netto CA, Wyse AT (2012) Chronic hyperhomocysteinemia increases inflammatory markers in hippocampus and serum of rats. Neurochem Res 37:1660–1669. https://doi.org/10.1007/s11064-012-0769-2

Figueiro PW, de SMD, Dos Santos TM, Prezzi CA, Rohden F, Faccioni-Heuser MC, Manfredini V, Netto CA, ATS W (2019) The neuroprotective role of melatonin in a gestational hypermethioninemia model. Int J Dev Neurosci 78:198–209. https://doi.org/10.1016/j.ijdevneu.2019.08.004

Frohman EM, Racke MK, Raine CS (2006) Multiple sclerosis – the plaque and its pathogenesis. N Engl J Med 354:942–955. https://doi.org/10.1056/NEJMra052130

Hague WM (2003) Homocysteine and pregnancy. Best Pract Res Clin Obstet Gynaecol 17:459–469

Heneka MT, Carson MJ, El Khoury J et al (2015) Neuroinflammation in Alzheimer's disease. Lancet Neurol 14:388–405. https://doi.org/10.1016/S1474-4422(15)70016-5

James SJ, Melnyk S, Pogribna M, Pogribny IP, Caudill MA (2002) Elevation in S-adenosylhomocysteine and DNA hypomethylation: potential epigenetic mechanism for homocysteine-related pathology. J Nutr 132:2361S–2366S. https://doi.org/10.1093/jn/132.8.2361S

Jha SK, Jha NK, Kar R, Ambasta RK, Kumar P (2015) p38 MAPK and PI3K/AKT signalling cascades in Parkinson's disease. Int J Mol Cell Med 4:67–86

Kasture VV, Sundrani DP, Joshi SR (2018) Maternal one carbon metabolism through increased oxidative stress and disturbed angiogenesis can influence placental apoptosis in preeclampsia. Life Sci 206:61–69. https://doi.org/10.1016/j.lfs.2018.05.029

Kim EK, Choi EJ (2015) Compromised MAPK signaling in human diseases: an update. Arch Toxicol 89:867–882. https://doi.org/10.1007/s00204-015-1472-2

Kovalska M, Hnilicova P, Kalenska D, Tothova B, Adamkov M, Lehotsky J (2019) Effect of methionine diet on metabolic and histopathological changes of rat hippocampus. Int J Mol Sci 20:6234. https://doi.org/10.3390/ijms20246234

Koz ST, Gouwy NT, Demir N, Nedzvetsky VS, Etem E, Baydas G (2010) Effects of maternal hyperhomocysteinemia induced by methionine intake on oxidative stress and apoptosis in pup rat brain. Int J Dev Neurosci 28:325–329. https://doi.org/10.1016/j.ijdevneu.2010.02.006

Kumar M, Sandhir R (2019) Hydrogen sulfide suppresses homocysteine-induced glial activation and inflammatory response. Nitric Oxide 90:15–28. https://doi.org/10.1016/j.niox.2019.05.008

Lee JK, Kim NJ (2017) Recent advances in the inhibition of p38 MAPK as a potential strategy for the treatment of Alzheimer's disease. Molecules 22:1287. https://doi.org/10.3390/molecules22081287

Longoni A, Kolling J, dos Santos TM, dos Santos JP, da Silva JS, Pettenuzzo L, Goncalves CA, de Assis AM, Quincozes-Santos A, Wyse AT (2016) 1,25-Dihydroxyvitamin D3 exerts neuroprotective effects in an ex vivo model of mild hyperhomocysteinemia. Int J Dev Neurosci 48:71–79. https://doi.org/10.1016/j.ijdevneu.2015.11.005

Longoni A, Bellaver B, Bobermin LD, Santos CL, Nonose Y, Kolling J, Dos Santos TM, de Assis AM, Quincozes-Santos A, Wyse ATS (2018) Homocysteine induces glial reactivity in adult rat astrocyte cultures. Mol Neurobiol 55:1966–1976. https://doi.org/10.1007/s12035-017-0463-0

Middeldorp J, Hol EM (2011) GFAP in health and disease. Prog Neurobiol 93:421–443. https://doi.org/10.1016/j.pneurobio.2011.01.005

Molnar Z, Clowry G (2012) Cerebral cortical development in rodents and primates. Prog Brain Res 195:45–70. https://doi.org/10.1016/B978-0-444-53860-4.00003-9

Moore AH, O'Banion MK (2002) Neuroinflammation and anti-inflammatory therapy for Alzheimer's disease. Adv Drug Deliv Rev 54:1627–1656. https://doi.org/10.1016/s0169-409x(02)00162-x

Morale MC, Serra PA, L'Episcopo F et al (2006) Estrogen, neuroinflammation and neuroprotection in Parkinson's disease: glia dictates resistance versus vulnerability to neurodegeneration. Neuroscience 138:869–878. https://doi.org/10.1016/j.neuroscience.2005.07.060

Murphy MM, Scott JM, Arija V, Molloy AM, Fernandez-Ballart JD (2004) Maternal homocysteine before conception and throughout pregnancy predicts fetal homocysteine and birth weight. Clin Chem 50:1406–1412. https://doi.org/10.1373/clinchem.2004.032904

Nijhawan D, Honarpour N, Wang X (2000) Apoptosis in neural development and disease. Annu Rev Neurosci 23:73–87. https://doi.org/10.1146/annurev.neuro.23.1.73

Ostrakhovitch EA, Tabibzadeh S (2019) Homocysteine and age-associated disorders. Ageing Res Rev 49:144–164. https://doi.org/10.1016/j.arr.2018.10.010

Palanca A, Casafont I, Berciano MT, Lafarga M (2014) Proteasome inhibition induces DNA damage and reorganizes nuclear architecture and protein synthesis machinery in sensory ganglion neurons. Cell Mol Life Sci 71:1961–1975. https://doi.org/10.1007/s00018-013-1474-2

Paxinos G, Watson C (2007) The rat brain in stereotaxic coordinates, sixth edn. Elsevier/Academic Press, New York

Poddar R, Paul S (2013) Novel crosstalk between ERK MAPK and p38 MAPK leads to homocysteine-NMDA receptor-mediated neuronal cell death. J Neurochem 124:558–570. https://doi.org/10.1111/jnc.12102

Poddar R, Chen A, Winter L, Rajagopal S, Paul S (2017) Role of AMPA receptors in homocysteine-NMDA receptor-induced crosstalk between ERK and p38 MAPK. J Neurochem 142:560–573. https://doi.org/10.1111/jnc.14078

Pustygina AV, Milyutina YP, Zaloznyaya IV, Arutyunyan AV (2015) Indices of oxidative stress in the brain of newborn rats subjected to prenatal hyperhomocysteinemia. Neurochem J 9:60–65. https://doi.org/10.1134/s1819712415010079

Riancho J, Ruiz-Soto M, Villagra NT, Berciano J, Berciano MT, Lafarga M (2014) Compensatory motor neuron response to chromatolysis in the murine hSOD1(G93A) model of amyotrophic lateral sclerosis. Front Cell Neurosci 8:346. https://doi.org/10.3389/fncel.2014.00346

Salissou MTM, Mahaman YAR, Zhu F, Huang F, Wang Y, Xu Z, Ke D, Wang Q, Liu R, Wang JZ, Zhang B, Wang X (2018) Methanolic extract of Tamarix Gallica attenuates hyperhomocysteinemia induced AD-like pathology and cognitive impairments in rats. Aging (Albany NY) 10:3229–3248. https://doi.org/10.18632/aging.101627

Sasi M, Vignoli B, Canossa M, Blum R (2017) Neurobiology of local and intercellular BDNF signaling. Pflugers Arch 469:593–610. https://doi.org/10.1007/s00424-017-1964-4

Scherer EB, Loureiro SO, Vuaden FC et al (2014) Mild hyperhomocysteinemia increases brain acetylcholinesterase and proinflammatory cytokine levels in different tissues. Mol Neurobiol 50:589–596. https://doi.org/10.1007/s12035-014-8660-6

Schweinberger BM, Rodrigues AF, Dos Santos TM, Rohden F, Barbosa S, da Luz Soster PR, Partata WA, Faccioni-Heuser MC, Wyse ATS (2018a) Methionine administration in pregnant rats causes memory deficit in the offspring and alters ultrastructure in brain tissue. Neurotox Res 33:239–246. https://doi.org/10.1007/s12640-017-9830-x

Schweinberger BM, Rodrigues AF, Turcatel E, Pierozan P, Pettenuzzo LF, Grings M, Scaini G, Parisi MM, Leipnitz G, Streck EL, Barbé-Tuana FM, Wyse ATS (2018b) Maternal hypermethioninemia affects neurons number, neurotrophins levels, energy metabolism, and Na(+),K(+)-ATPase expression/content in brain of rat offspring. Mol Neurobiol 55:980–988. https://doi.org/10.1007/s12035-017-0383-z

Selhub J (1999) Homocysteine metabolism. Annu Rev Nutr 19:217–246. https://doi.org/10.1146/annurev.nutr.19.1.217

Shafqat N, Muniz JR, Pilka ES, Papagrigoriou E, von Delft F, Oppermann U, Yue WW (2013) Insight into S-adenosylmethionine biosynthesis from the crystal structures of the human methionine adenosyltransferase catalytic and regulatory subunits. Biochem J 452:27–36. https://doi.org/10.1042/BJ20121580

Shcherbitskaya AD, Milyutina YP, Zaloznyaya IV, Arutjunyan AV, Nalivaeva NN, Zhuravin IA (2017) The effects of prenatal hyperhomocysteinemia on the formation of memory and the contents of biogenic amines in the rat hippocampus. Neurochem J 11:296–301. https://doi.org/10.1134/s1819712417040080

Sibarov DA, Abushik PA, Giniatullin R, Antonov SM (2016) GluN2A subunit-containing NMDA receptors are the preferential neuronal targets of homocysteine. Front Cell Neurosci 10:246. https://doi.org/10.3389/fncel.2016.00246

Song Q, Fan C, Wang P, Li Y, Yang M, Yu SY (2018) Hippocampal CA1 betaCaMKII mediates neuroinflammatory responses via COX-2/PGE2 signaling pathways in depression. J Neuroinflammation 15:338. https://doi.org/10.1186/s12974-018-1377-0

Stojkovska I, Wagner BM, Morrison BE (2015) Parkinson's disease and enhanced inflammatory response. Exp Biol Med 240:1387–1395. https://doi.org/10.1177/1535370215576313

Tsitsiou E, Sibley CP, D'Souza SW, Catanescu O, Jacobsen DW, Glazier JD (2011) Homocysteine is transported by the microvillous plasma membrane of human placenta. J Inherit Metab Dis 34:57–65. https://doi.org/10.1007/s10545-010-9141-3

van der Bruggen T, Nijenhuis S, van Raaij E, Verhoef J, van Asbeck BS (1999) Lipopolysaccharide-induced tumor necrosis factor alpha production by human monocytes involves the raf-1/MEK1-MEK2/ERK1-ERK2 pathway. Infect Immun 67:3824–3829

Vasilev DS, Tumanova NL, Kim KK, Lavrentyeva VV, Lukomskaya NY, Zhuravin IA, Magazanik LG, Zaitsev AV (2018) Transient morphological alterations in the hippocampus after pentylenetetrazole-induced seizures in rats. Neurochem Res 43:1671–1682. https://doi.org/10.1007/s11064-018-2583-y

Wan L, Sun Y, Zhang F, Ren Y (2016) Low-dose homocystine enhances proliferation and migration of Bv2 microglia cells. Cell Mol Neurobiol 36:1279–1289. https://doi.org/10.1007/s10571-015-0325-0

Wang X, Li W, Li S, Yan J, Wilson JX, Huang G (2018) Maternal folic acid supplementation during pregnancy improves neurobehavioral development in rat offspring. Mol Neurobiol 55:2676–2684. https://doi.org/10.1007/s12035-017-0534-2

Weekman EM, Woolums AE, Sudduth TL, Wilcock DM (2017) Hyperhomocysteinemia-induced gene expression changes in the cell types of the brain. ASN Neuro 9:1759091417742296. https://doi.org/10.1177/1759091417742296

Weekman EM, Sudduth TL, Price BR, Woolums AE, Hawthorne D, Seaks CE, Wilcock DM (2019) Time course of neuropathological events in hyperhomocysteinemic amyloid depositing mice reveals early neuroinflammatory changes that precede amyloid changes and cerebrovascular events. J Neuroinflammation 16:284. https://doi.org/10.1186/s12974-019-1685-z

Wojtera M, Sikorska B, Sobow T, Liberski PP (2005) Microglial cells in neurodegenerative disorders. Folia Neuropathol 43:311–321

Wu B, Yue H, Zhou GH, Zhu YY, Wu TH, Wen JF, Cho KW, Jin SN (2019) Protective effects of oxymatrine on homocysteine-induced endothelial injury: involvement of mitochondria-dependent apoptosis and Akt-eNOS-NO signaling pathways. Eur J Pharmacol 864:172717. https://doi.org/10.1016/j.ejphar.2019.172717

Yasuda S, Sugiura H, Tanaka H, Takigami S, Yamagata K (2011) p38 MAP kinase inhibitors as potential therapeutic drugs for neural diseases. Cent Nerv Syst Agents Med Chem 11:45–59. https://doi.org/10.2174/187152411794961040

Yi P, Melnyk S, Pogribna M, Pogribny IP, Hine RJ, James SJ (2000) Increase in plasma homocysteine associated with parallel increases in plasma S-adenosylhomocysteine and lymphocyte DNA hypomethylation. J Biol Chem 275:29318–29323. https://doi.org/10.1074/jbc.M002725200

Zhu Z, Ge M, Li C, Yu L, Gu Y, Hu Y, Cao Z (2020) Effects of p38 MAPK signaling pathway on cognitive function and recovery of neuronal function after hypoxic-ischemic brain injury in newborn rats. J Clin Neurosci. https://doi.org/10.1016/j.jocn.2020.04.085

Zou CG, Zhao YS, Gao SY, Li SD, Cao XZ, Zhang M, Zhang KQ (2010) Homocysteine promotes proliferation and activation of microglia. Neurobiol Aging 31:2069–2079. https://doi.org/10.1016/j.neurobiolaging.2008.11.007